10.1071/FP13033_AC



Supplementary Material: *Functional Plant Biology*, 2014, 41(1), 37–47.

## Supplementary Material

# The role of leaf hydraulic conductance dynamic on the timing of leaf senescence

*Juan Pablo Giraldo*[A,B], *James K. Wheeler*[A], *Brett A. Huggett*[A] *and N. Michele Holbrook*[A]

[A]Harvard University, Department of Organismic and Evolutionary Biology, 16 Divinity Avenue. Biolabs Rm 3107, Cambridge, MA 02138, USA.

[B]Corresponding author. Email: jgiraldo@post.harvard.edu

**Supplementary materials and methods**

*Tomato plant material*

Wildtype var. MP-1 tomato plants (*Solanum lycopersicum*) were grown in a glasshouse at 13 hour day length with supplementary light, 25 °C day and 20 °C night, and relative humidity ranging from 30 to 80%. Soil was watered daily and fertilized with Osmocote pellets and a 20-10-20 Peat Lite Special Solution (Peters Professional). Flower buds were removed regularly to avoid leaf senescence induced by reproductive status. All lateral branches were cut off, leaving only the leaves attached directly to the leading shoot and thus having the same vascular supply. Plants were spaciously distributed in the glasshouse. Measurements were performed when plants were between two to three months old and had at least 16 nodes. Sampled leaves for $K_{leaf}$, and gas exchange, were attached to the leading shoot at the following leaf nodes from the plant apex (LNA): 4, 7, 9, 11, 13, and 15. A set of five plants was used to determine the relationship between average leaf age and LNA. Leaves were labeled with date of leaf flushing and leaf age calculated as the time interval between labeling and recording of LNA when individuals had at least 16 nodes. The resulting linear regression, Leaf age (days) = 2.33 * LNA - 2.94 ($R^2$ = 0.9694, $P < 0.001$, n = 6), was then used to determine the average leaf age based on LNA. To understand the underlying causes leading to $K_{leaf}$ decline with age, we studied leaflet and rachis hydraulic dynamics in compound tomato leaves. Rachis was identified as the main leaf axis to which all leaflets are attached. Selected young (13 days) and old leaves (27 days) were connected to the main stem at nodes $7^{th}$ and $13^{th}$, respectively, from the plant apex. Leaves were measured for leaflet and rachis hydraulic conductance, petiole xylem cross sectional area, vessel size distribution, and percent loss of conductance.

*Leaf chlorophyll content*

A significant decline in leaf chlorophyll content was used as an indicator of the onset of leaf senescence. Leaf chlorophyll absorbance was measured *in situ* with a SPAD meter (Minolta, SPAD 502) as the average of 4 to 11 leaves or leaflets per individual taken at random locations on the leaf lamina. To calibrate the SPAD readings, total chlorophyll content (A + B) was measured by spectrophotometry (Lee, O'Keefe *et al.* 2003). In brief, leaf punches (0.3848 $cm^2$) were taken from leaves of three to five individuals with a wide range of chlorophyll SPAD absorbances from senescing to young leaves. The leaf punches were submerged in N,N-Dimethyl formamide (Sigma) and placed in the dark at a temperature of 5 °C for at least 48 hours. Chlorophyll absorbance was

measured with a spectrophotometer (Varian Inc., Cary model 219 and UV-2100U, Shimadzu) and chlorophyll content calculated using the equations for 0.2 nm wavelength bandwidth as in Wellburn (1994). Linear regressions were used to convert SPAD chlorophyll absorbance measurements to chlorophyll A+B content (μg $cm^{-2}$): for tomato Chl A+B = 0.90 * Chl SPAD - 4.58 ($R^2$ = 0.961, P < 0.01), *A. excelsum* **C**hl A+B = - 13.77 +1.56 * Chl SPAD ($R^2$ = 0.718, P < 0.01), for *A. trichanta* **C**hl A+B = - 29.14 +1.76 * Chl SPAD ($R^2$ = 0.863, P < 0.01), for *A. saccharum* Chl A+B = 1.62 * Chl SPAD - 24.45 ($R^2$ = 0.933, P < 0.01) and for *Q. rubra* Chl A+B = 1.68 * Chl SPAD - 17.94 ($R^2$ = 0.951, P < 0.01) (Fig. S1).

*Tomato leaflet and rachis hydraulic conductance*

The hydraulic conductance of the most apical leaflet ($K_{leaflet}$) was measured by the evaporative flux method using a flowmeter as described above (Brodribb and Holbrook 2006). Leaflet lamina temperatures from 32 to 35 °C were recorded with an infrared detector (Omega, OS543). Relative humidity near the leaflet surface ranged between 27 to 41 % (McMaster-Carr, Digital sling psychrometer SAM990DW). Leaf specific rachis hydraulic conductance was determined with a flowmeter (Brodribb and Holbrook 2006). Rachis was cut with a razor blade by submerging underwater to prevent the formation of embolisms. All leaflets were excised with only the rachis remaining. The rachis was immediately attached via silicone and tygon tubing to a water reservoir (IV bag) generating a driving pressure from 1.44 to 2.25 kPa (Omega, PX-26). Leaf specific rachis hydraulic conductance was calculated as $K_{rachis}$ = Flow / Driving pressure, normalized by leaf area supplied by the rachis (LI-1300).

*Tomato percent loss of petiole conductance*

The most basal segment of the rachis between the main plant axis and the first petiolule (hereafter referred to as the petiole) was excised underwater with a clean razor blade. The petiole was immediately attached to the flowmeter system and flow values measured similarly to those described above. Driving pressures across the petiole were under 1.7 kPa to avoid refilling open vessels. After the native flow ($F_{native}$) reading was recorded the petiole was flushed by pushing filtered (Pall Acrodisc, 0.2 μm mesh syringe filter) and deionized water at approximately 200 kPa into one end for 30 seconds. Flow values were recorded again under the original driving pressure to determine maximum petiole flow ($F_{max}$). Percent loss of conductance was calculated as PLC = (1 - ($F_{native}$ / $F_{max}$)) * 100.

*Diameter distribution of petiole conductive vessels in tomato*

To determine the size distribution of conductive vessels in the petiole of young and old leaves we performed leaf live staining with acid fuchsin. Leaves were connected to a clear tygon tubing (1/8 inch ID) filled with a solution of 0.2% acid fuchsin filtered beforehand with a 0.2 µm membrane (Pall Acrodisc, syringe filter). Transpiration was induced for one hour under a halogen lamp as explained above. The first 2.5 cm of the petiole downstream from the stain feeding point was discarded to avoid dye diffusion artifacts in the non-vascular tissue. Petiole segments were sectioned as explained above. Sections were observed using a compound microscope (Olympus, BH-2) and an image taken of the third xylem quadrant starting from the top of the petiole in a clockwise direction, with a digital camera (Zeiss, Axiocam HRc) at 10X magnification. Camera imaging software (Axiovision 4.3) HUE parameters and exposure time were set as automatic. Vessels were outlined in ImageJ (NIH) by setting color threshold plugin in the CIE Lab mode with a* = 128 to filter only the acid fuchsin stained parts of the xylem, after which the freehand selection tool was used to trace the cell walls of all stained xylem vessels. Vessel cell wall traces were measured for area, perimeter, major and minor axis dimensions.

*Environmental conditions of canopy humidity and control chambers*

Diurnal measurements of PAR, relative humidity, ambient and leaf temperature were performed on sunny days in both high humidity and control chambers. Maximum PAR on the leaf surface was measured with a light meter (LICOR, LI-250). High humidity and air temperature were monitored using a portable psychrometer (McMaster-Carr, Digital sling psychrometer SAM990DW), and leaf temperature recorded with an infrared sensor (Omega, OS543). Vapor pressure deficit was calculated as $VPD = e_s - e$ where the saturated vapor pressure $e_s = 0.61365 * e^{(17.502*T) / (240.97+T)}$ and the actual vapor pressure $e = e_s * RH / 100$. Quantum yield and electron transport rate light curves were determined with a Mini-Pam (Walz) to assess the effect of the high humidity treatment on photosynthetic light reactions. In sunny mornings, light adapted leaves in both high humidity and control chambers were exposed to increasing levels of PAR for a period of 10 seconds followed by a measurement of QY and ETR.

## References

Brodribb TJ, Holbrook NM (2006) Declining hydraulic efficiency as transpiring leaves desiccate: two types of response. *Plant Cell and Environment* **29**, 2205–2215.

Lee DW, O'Keefe J, Holbrook NM, Feild TS (2003) Pigment dynamics and autumn leaf senescence in a New England deciduous forest, eastern USA. *Ecological Research* **18**, 677–694.

Sack L, Melcher PJ, Zwieniecki MA, Holbrook NM (2002) The hydraulic conductance of the angiosperm leaf lamina: A comparison of three measurement methods. *Journal of Experimental Botany* **53**, 2177–2184.

Wellburn AR (1994) The spectral determination of chlorophyll-a and chlorophyll-b, as well as total carotenoids, using various solvents with spectrophotometers of different resolution. *Journal of Plant Physiology* **144**, 307–313.

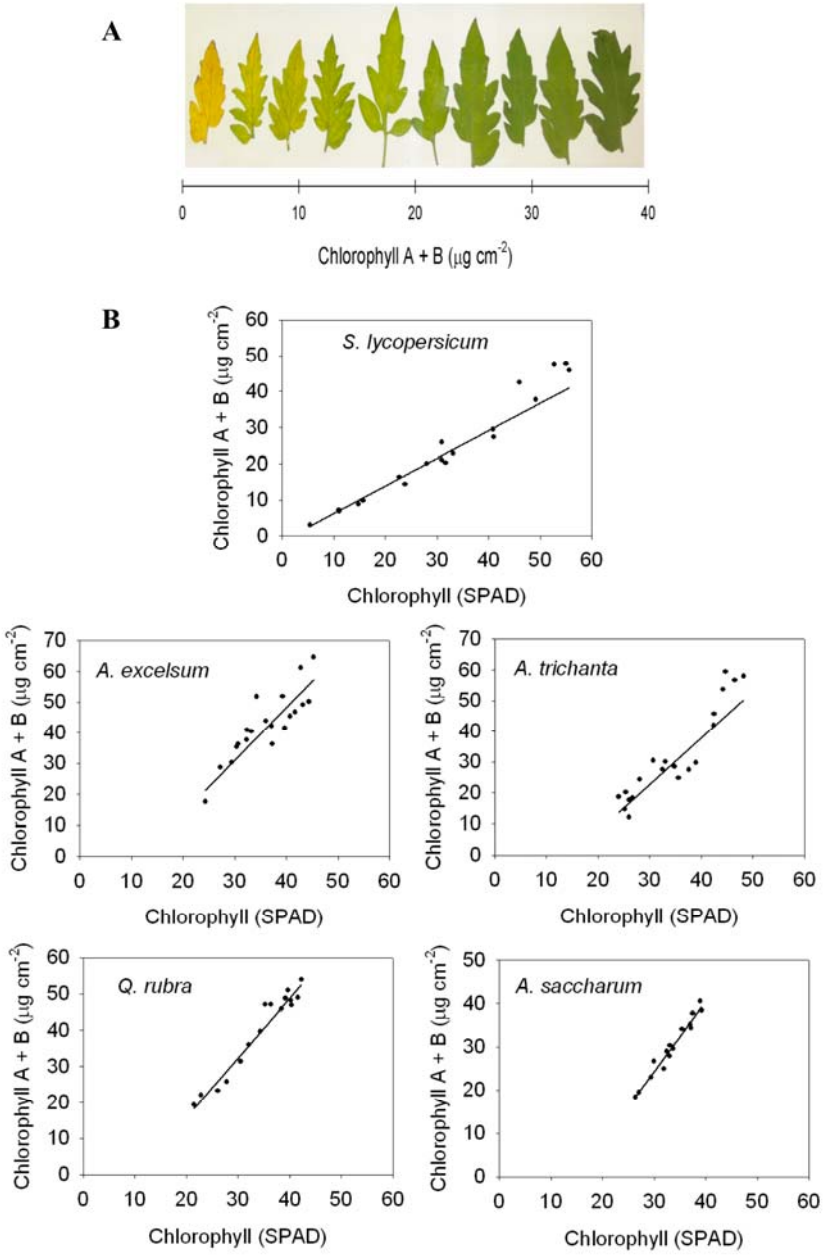


**Fig. S1.** (A) Chlorophyll content scale from senesced (left) to young leaves (right) of *S. lycopersicum*. (B) Leaf chlorophyll absorbance was measured with a SPAD meter in random areas on the leaf lamina and chlorophyll content values calculated from linear regressions ($n$ = 3–5).

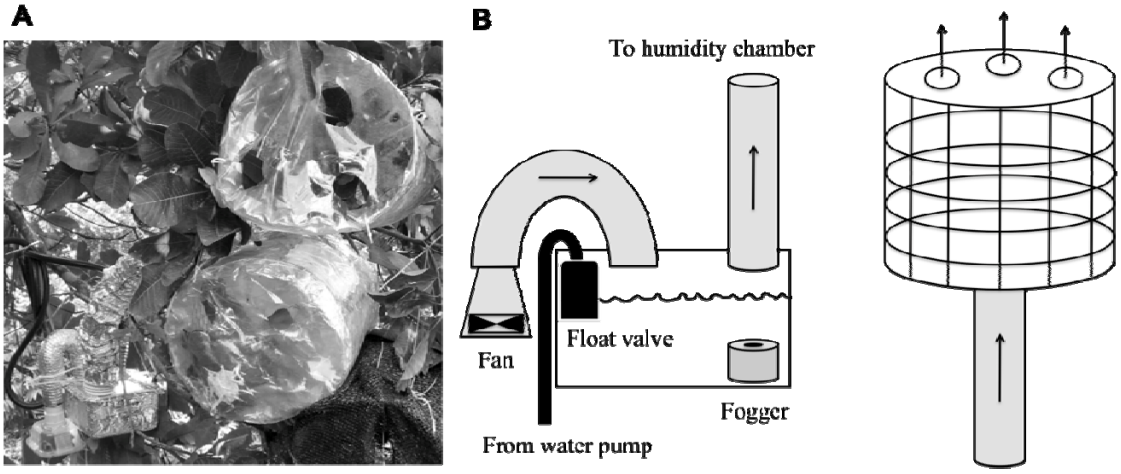


**Fig. S2.** (A) From top to bottom: canopy control and humidity chambers on an *A. excelsum* tree around the STRI canopy crane. (B) High humidity chambers consisted of clear plastic wrapped metal frames connected to an airtight acrylic box containing a fogger (MICO Inc, M001) submerged in water. A 12 V DC fan (McMaster-Carr) blew air at saturated vapor pressure via air conditioner flexible hose. Acrylic box and air hoses were covered with aluminum foil and duct tape. Water was supplied through a garden hose connected to a water pump located at ground level. Water levels were regulated inside the acrylic box with a tank float valve (Dare products Inc.). All chambers had small openings at the top to allow free air circulation.

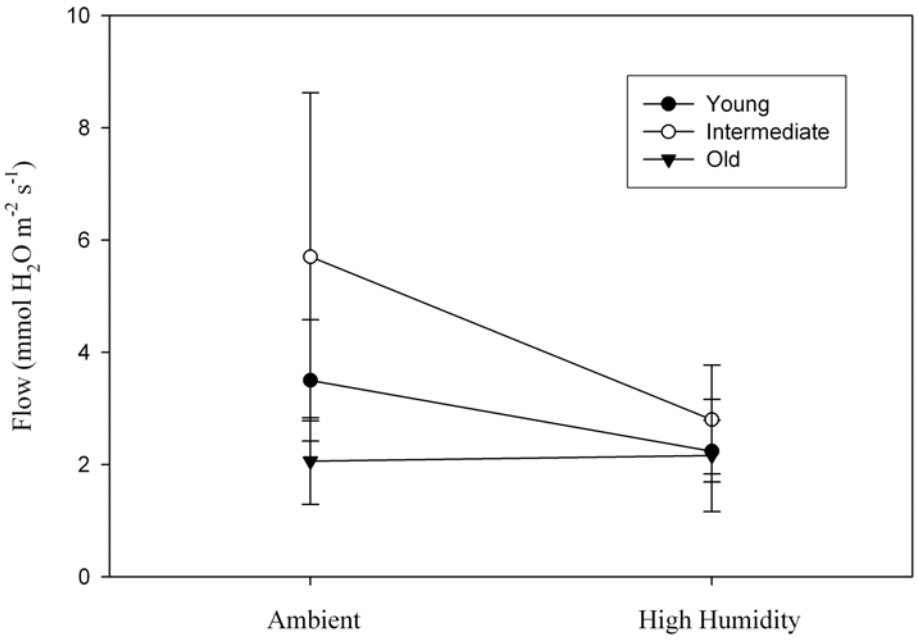


**Fig. S3.** Flow values recorded with a flowmeter in excised *S. lycopersicum* leaves under canopy humidity and control chamber conditions ($n$ = 6).

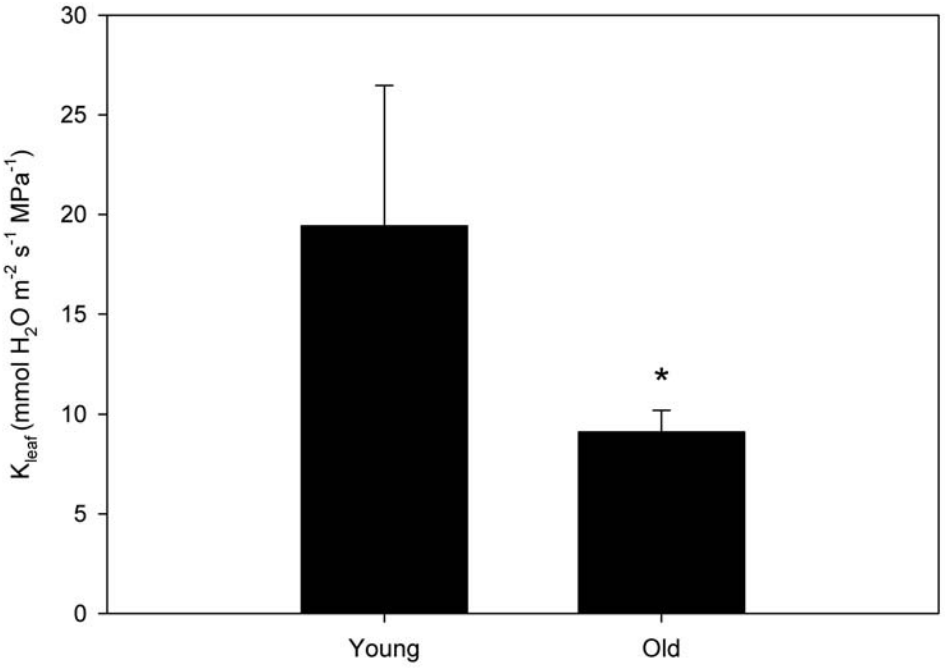


**Fig. S4.** Decline in hydraulic conductance of leaves at a fixed node from the base of the plant (*t*-test, $P < 0.05$). Young and old leaves were separated by a 25-day difference in age. Young leaves were at LNA 5 to 6 and old leaves at LNA 12 to 14. Data are averages plus or minus standard deviation ($n$ = 5–6).

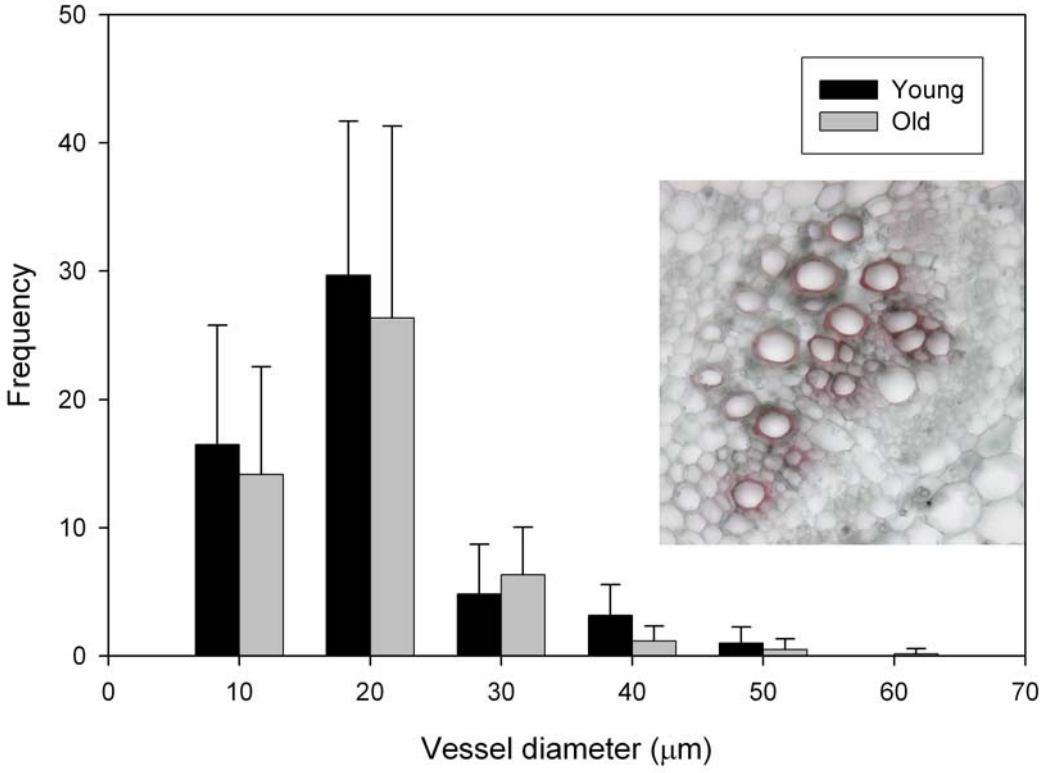


**Fig. S5.** Diameter distribution of conductive xylem vessels in young (LNA 7) and old (LNA 13) leaves. Bars represent average counts of vessels stained by acid fuchsin in transpiring leaves for each size category plus or minus standard deviations ($n$ = 5). No significant differences were found between leaf ages within each category with 95% confidence ($t$-test).

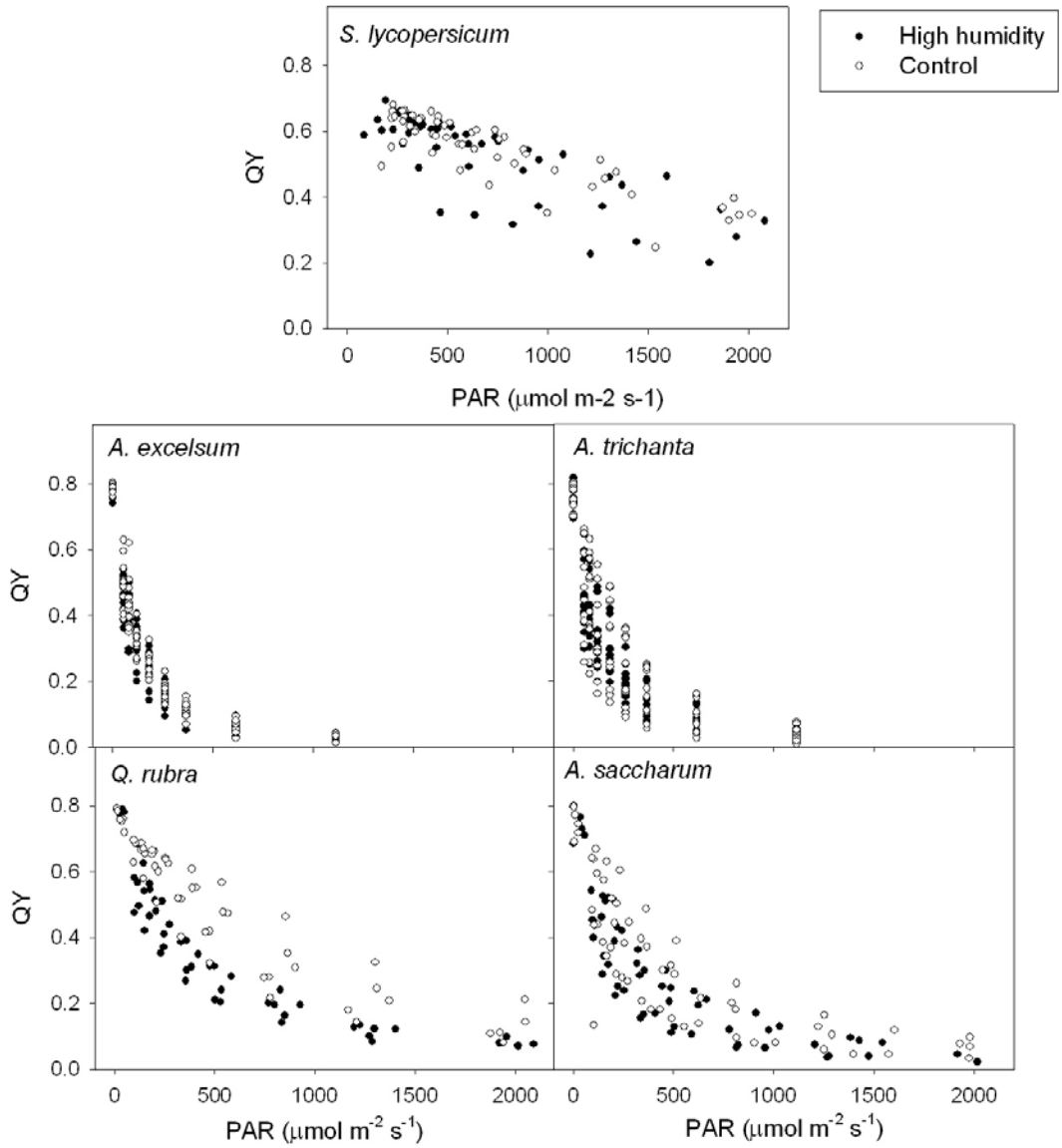


**Fig. S6.** Quantum yield (QY) light curves for leaves in high humidity and control chambers (*n* = 3–5). Measurements were taken in light adapted leaves.

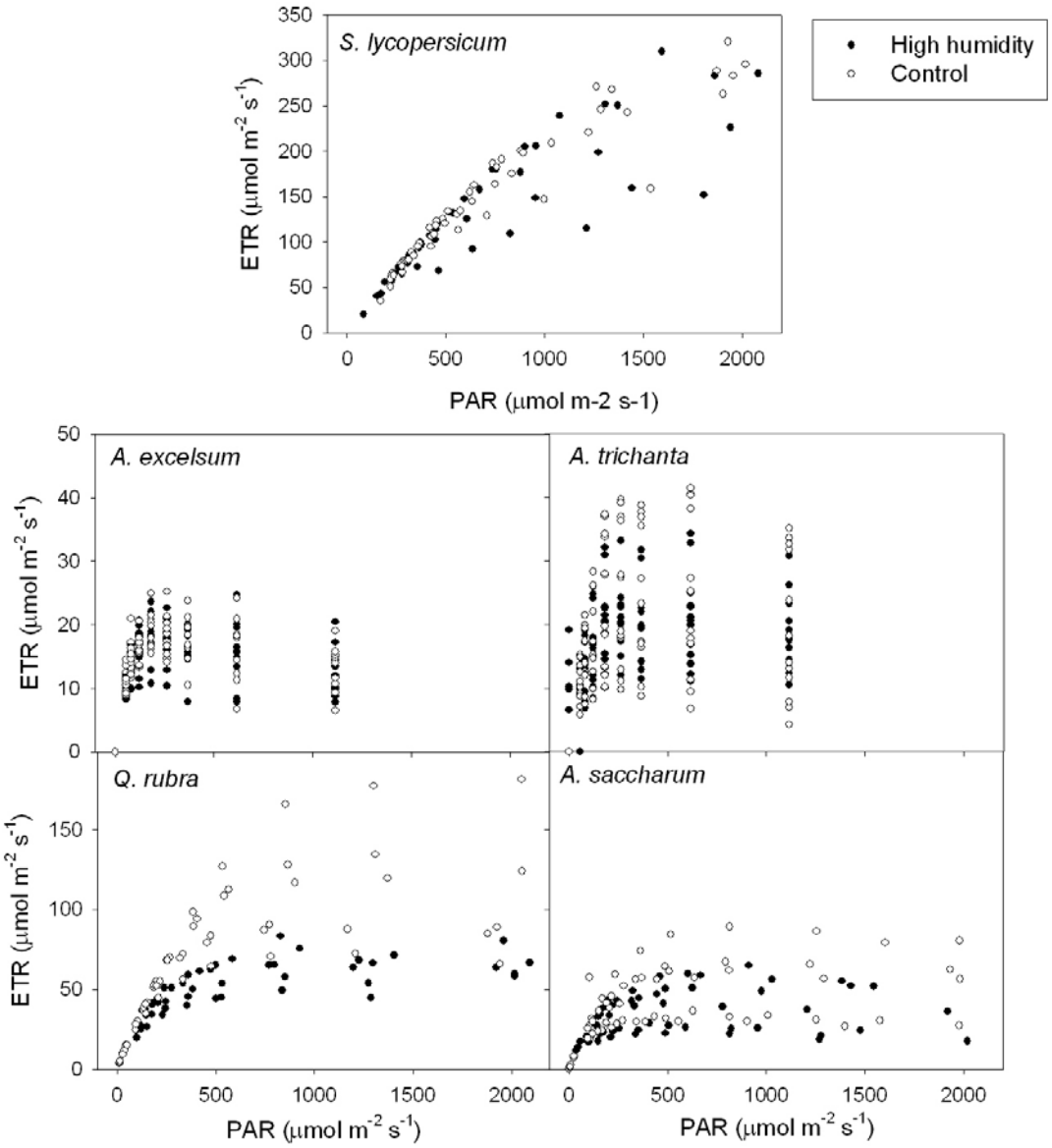


**Fig. S7.** Electron transport rates (ETR) light curves for leaves in high humidity and control chambers ($n$ = 3–5). Measurements were taken in light adapted leaves.

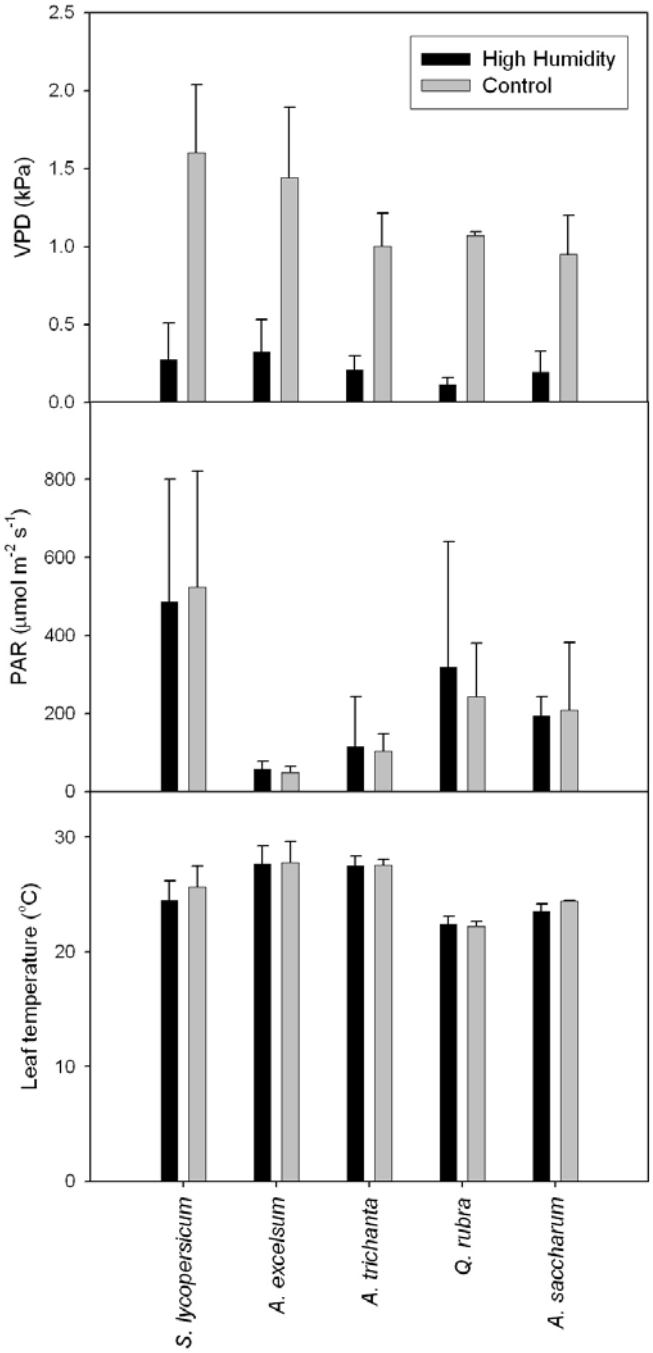


**Fig. S8.** Diurnal patterns of vapor pressure deficit (VPD), photosynthetically active radiation (PAR), air temperature and leaf temperature in high humidity and control treatments ($n$ = 3–5).